HHS Public Access

Author manuscript

Cell Rep. Author manuscript; available in PMC 2022 May 11.

Published in final edited form as:

Cell Rep. 2022 April 12; 39(2): 110655. doi:10.1016/j.celrep.2022.110655.

A Zika virus mutation enhances transmission potential and confers escape from protective dengue virus immunity

Jose Angel Regla-Nava[1,6], **Ying-Ting Wang**[1], **Camila R. Fontes-Garfias**[2], **Yang Liu**[2], **Thasneem Syed**[1], **Mercylia Susantono**[1], **Andrew Gonzalez**[1], **Karla M. Viramontes**[1], **Shailendra Kumar Verma**[1], **Kenneth Kim**[1], **Sara Landeras-Bueno**[1], **Chun-Teng Huang**[3], **Daniil M. Prigozhin**[4], **Joseph G. Gleeson**[5], **Alexey V. Terskikh**[3], **Pei-Yong Shi**[2,*], **Sujan Shresta**[1,7,*]

[1]Center for Infectious Disease and Vaccine Research, La Jolla Institute for Immunology, La Jolla, CA 92037, USA

[2]Department of Biochemistry and Molecular Biology, Sealy Institute for Drug Discovery, Department of Pharmacology and Toxicology and Sealy Center for Structural Biology and Molecular Biophysics, University of Texas Medical Branch, Galveston, TX 77555, USA

[3]Sanford Burnham Prebys Medical Discovery Institute, La Jolla, CA 92037, USA

[4]Molecular Biophysics and Integrative Bioimaging Division, Lawrence Berkeley National Laboratory, Berkeley, CA 94720, USA

[5]Howard Hughes Medical Institute, Rady Children's Institute of Genomic Medicine, Department of Neurosciences, University of California, San Diego, San Diego, CA 92093, USA

[6]Present address: Department of Microbiology and Pathology, University Center for Health Science (CUCS), University of Guadalajara, Guadalajara 44340, Mexico

[7]Lead contact

SUMMARY

Zika virus (ZIKV) and dengue virus (DENV) are arthropod-borne pathogenic flaviviruses that co-circulate in many countries. To understand some of the pressures that influence ZIKV evolution, we mimic the natural transmission cycle by repeating serial passaging of ZIKV through cultured mosquito cells and either DENV-naive or DENV-immune mice. Compared with wild-type ZIKV, the strains passaged under both conditions exhibit increased pathogenesis in DENV-immune mice. Application of reverse genetics identifies an isoleucine-to-valine mutation (I39V) in the NS2B

*Correspondence: peshi@utmb.edu (P.-Y.S.), sujan@lji.org (S.S.).

AUTHOR CONTRIBUTIONS

J.A.R.-N. and S.S. conceived the project. J.A.R.-N., Y.-T.W., C.R.F.-G., Y.L., C.-T.H., T.S., M.S., A.G., K.M.V., S.V., K.K., D.M.P., and S.L. performed the experiments and analyzed the data. J.G.G., A.V.T., P.-Y.S., and S.S. obtained funding and designed the experiments. S.S. supervised the research. S.S. wrote the manuscript and other authors provided editorial comments.

DECLARATION OF INTERESTS

The authors declare no conflicts of interest.

SUPPLEMENTAL INFORMATION

Supplemental information can be found online at https://doi.org/10.1016/j.celrep.2022.110655.

proteins of both passaged strains that confers enhanced fitness and escape from pre-existing DENV immunity. Introduction of I39V or I39T, a naturally occurring homologous mutation detected in recent ZIKV isolates, increases the replication of wild-type ZIKV in human neuronal precursor cells and laboratory-raised mosquitoes. Our data indicate that ZIKV strains with enhanced transmissibility and pathogenicity can emerge in DENV-naive or -immune settings, and that NS2B-I39 mutants may represent ZIKV variants of interest.

In brief

Regla-Nava et al. find that serial passaging of ZIKV strain *in vitro/in vivo* produces a single mutation that is sufficient to enhance ZIKV virulence and escape the protective effects of pre-existing DENV immunity. NS2B I39V/I39T mutation significantly increases infectivity in human fetal NPCs and mosquitoes and enhanced pathogenicity in mice.

Graphical Abstract

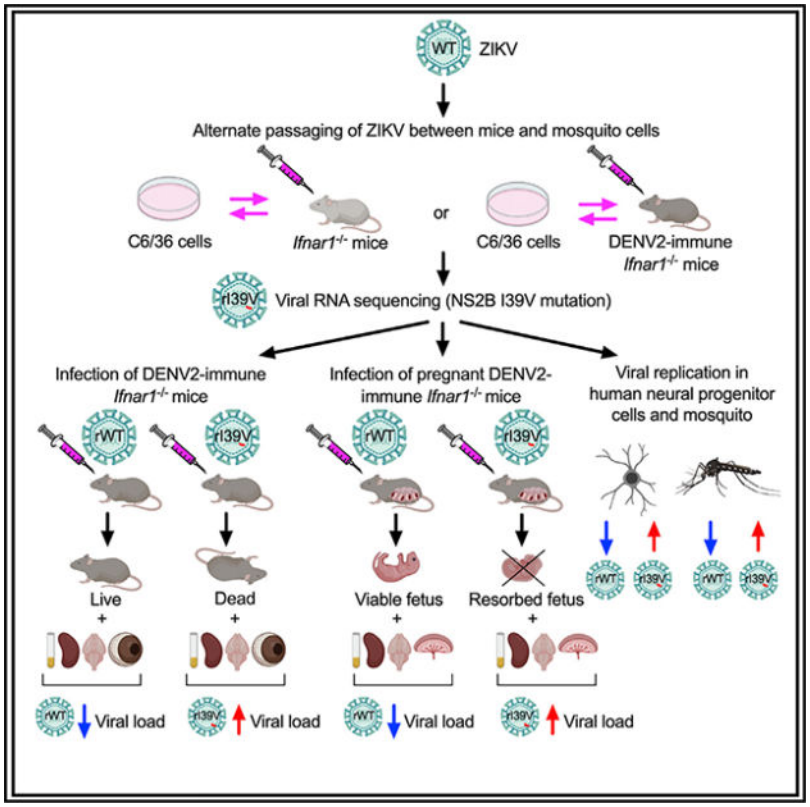

INTRODUCTION

Zika virus (ZIKV) and dengue virus (DENV) are closely related members of the Flaviviridae family of positive-stranded RNA viruses that also includes West Nile virus (WNV), yellow fever virus (YFV), and Japanese encephalitis virus (JEV) (Pierson and Diamond, 2020). ZIKV was first isolated in Uganda in 1947 and circulated in obscurity for decades until its emergence as the cause of the 2015 epidemic in Latin America (Faria et al., 2017; Musso

and Gubler, 2016). Since then, ZIKV has spread throughout the globe and is especially prevalent in DENV-endemic regions; consequently, the two flaviviruses now co-circulate in many countries (Rico-Mendoza et al., 2019; Rodriguez-Morales et al., 2016). ZIKV and DENV share the same primary vector, *Aedes aegypti* mosquitoes, and ZIKV can also be transmitted vertically from mothers to offspring and horizontally via sexual transmission (Besnard et al., 2014; Major et al., 2021). In both animal models and humans, ZIKV can persist in the semen, testes, and female reproductive tract for several months after infection (Mansuy et al., 2016; Tang et al., 2016b). Although the majority of ZIKV and DENV infections are asymptomatic or cause only mild symptoms such as fever, rash, and headache, both viruses can induce severe and life-threatening conditions, including congenital Zika syndrome and Guillain–Barré syndrome in the case of ZIKV infection and hemorrhagic fever and fatal shock in the case of DENV infection (Bhatt et al., 2013; Peixoto et al., 2019; Rasmussen et al., 2016).

ZIKV and the four serotypes of DENV (DENV1–4) share ~43% overall amino acid sequence identity and up to 56% and 68% identity in their envelope (E) and nonstructural (NS) proteins, respectively (Lazear and Diamond, 2016; Wen and Shresta, 2019). Such antigenic similarity leads to cross-reactive antibody (Ab)-mediated and T cell-mediated immunity, which has been well-documented *in vitro* as well as in mouse models of flaviviral infection and in humans. Much attention has been paid to the immunological and clinical consequences of DENV/ZIKV infection in individuals with cross-reactive immunity to the reciprocal virus (Elong Ngono and Shresta, 2018, 2019). Epidemiological modeling in humans and studies in mice have shown that pre-existing DENV immunity can cross-protect against ZIKV infection; however, the fact that both viruses co-circulate suggests that ZIKV has evolved mechanisms to escape the restrictions conferred by pre-existing DENV immunity. Comparison of the amino acid sequences of ZIKV strains circulating before and after the 2015 epidemic identified some changes that have been demonstrated to alter ZIKV virulence and transmission in animal models and laboratory mosquitoes. For example, mutation of alanine (A) 188 to valine (V) in the nonstructural protein NS1 was shown to enhance ZIKV infectivity and prevalence in laboratory *A. aegypti* mosquitoes (Liu et al., 2017) and to inhibit type I interferon (IFN) production in human cells and mice (Xia et al., 2018). Similarly, mutation of the precursor membrane protein (prM) serine (S) 139 to asparagine (N) increased ZIKV infectivity in human and mouse neural progenitor cells (NPCs) and severity of disease in mice (Yuan et al., 2017). Mutation of V473 to methionine (M) in the E protein increased ZIKV transplacental transmission and neurovirulence in mice (Shan et al., 2020). These findings suggest that acquisition of genetic changes that enhance ZIKV infection in humans and/or mosquitoes might have triggered the 2015 outbreak. They also highlight the potential for more virulent strains of ZIKV to emerge in the future, particularly given the high mutation frequencies of viral RNA-dependent RNA polymerases. However, little is known about how ZIKV evolution is affected by adaptation in mosquitoes or humans, or by the pressures of pre-existing immunity to DENV, both of which are particularly relevant for predicting possible outbreaks in regions where a large proportion of the population has been exposed to DENV.

To understand the mechanisms by which these factors influence ZIKV virulence and transmissibility, we examined ZIKV strains that had been serially passaged through cultured

mosquito cells and either DENV-naive or DENV2-immune mice. The resulting ZIKV strains were then examined for sequence mutations. Using reverse genetics, we introduced the mutations of interest and we examined their impact on ZIKV infectivity, transmissibility, and pathogenicity in cultured human and mosquito cells, non-pregnant and pregnant IFN-α/β receptor-deficient (*Ifnar1*$^{-/-}$) mice, and *A. aegypti* mosquitoes. We identified a single substitution, NS2B I39V, that enhanced ZIKV virulence in the presence of pre-existing DENV2 immunity. Notably, recombinant ZIKV strains harboring either I39V or a homologous I39-to-threonine (T) mutation, which was identified in recent clinical isolates, resulted in enhanced ZIKV virulence in mice and transmission in laboratory mosquitoes. Our data thus suggest that the emergence of ZIKV strains with NS2B-I39 mutations should be monitored as variants of interest with the potential for enhanced transmission and/or virulence in humans.

RESULTS

Mimicking of natural ZIKV evolution by passaging through mosquito cells and mice increases ZIKV virulence

To explore how ZIKV might evolve during its natural transmission cycle in both DENV-naive and DENV-immune hosts, we generated two new ZIKV strains by alternate passaging of wild-type (WT) ZIKV FSS13025 (2010 Cambodian isolate) between cultured *Aedes albopictus* C6/36 mosquito cells and either naive or DENV2-immune *Ifnar1*$^{-/-}$ mice (Figure S1A). In brief, groups of naive or DENV2-immune *Ifnar1*$^{-/-}$ mice (infected 30 days prior with 10^3 focus-forming units [FFU] of DENV2 strain S221) were infected via intravenous (i.v.) injection with 10^4 FFU of WT ZIKV and bled 3 days post-infection (dpi). The sera were then added to cultured C6/36 cells for an additional 7 to 10 days, and the viruses were harvested and injected i.v. into new groups of naive or DENV2-immune *Ifnar1*$^{-/-}$ mice. This cycle was repeated a total of 10 times, and the resulting ZIKV strains passaged through naive and DENV-immune mice were designated ZN-p10 and ZDI-p10, respectively (Figure S1A). Of note, sera, rather than tissues, from infected mice were used for passaging because sera contain transmissible virus.

To evaluate whether passaging affected ZIKV virulence, we infected 8- to 9-week-old naive or DENV2-immune female *Ifnar1*$^{-/-}$ mice via intra-footpad (IF) injection with vehicle (PBS/10% FBS) or 10^4 FFU of WT ZIKV, ZN-p10, or ZDI-p10, and compared the clinical phenotypes and viral burden in selected tissues. Naive mice were equally susceptible to infection with WT ZIKV, ZN-p10, and ZDI-p10 strains, and they displayed comparable disease severity and mortality rates (Figures 1A–1C). However, although the DENV2-immune *Ifnar1*$^{-/-}$ mice were protected against infection with WT ZIKV, consistent with our previous observations (Regla-Nava et al., 2018; Wen et al., 2017a), the mice were susceptible to fatal infection with both ZN-p10 and ZDI-p10; both strains induced severe disease at about 4 dpi and were 100% lethal by 9 dpi (Figures 1E–1G). Disease onset and mortality in DENV2-immune mice were accelerated to a small but significant extent after infection with ZDI-p10 compared with ZN-p10. Thus, passaging through either naive or DENV2-immune mice markedly increases ZIKV virulence.

To determine whether the increased pathogenicity of ZN-p10 and ZDI-p10 strains resulted from enhanced viral replication levels, we measured infectious viral particles in the serum, spleen, brain, and eyes of infected mice at 3 dpi using focus-forming assays (FFAs). In both naive and DENV2-immune ZIKV-infected mice, higher viral loads were detected after infection with ZN-p10 or ZDI-p10 compared with WT ZIKV (Figures 1D and 1H), indicating that the increased pathogenicity of passaged ZIKV was at least partly due to an increase in viral replication levels. Of note, the magnitude and kinetics of WT ZIKV, ZN-p10, and ZDI-p10 infection of C6/36 cells and mammalian Vero cells *in vitro* did not differ significantly (Figure S1B), suggesting that the replication-related phenotypes of passaged ZIKV might be cell-type dependent. Next, we sequenced ZIKV, ZN-p10, and ZDI-p10 to identify potential alterations responsible for the increased virulence of the ZIKV-passaged strains. At the level of viral consensus genomes, we detected two mutations in ZN-p10; one was a synonymous cytosine-to-uracil mutation (C1742U) in the sequence encoding the E protein, and the second was a non-synonymous adenosine-to-guanosine (A4338G) mutation resulting in a conservative I39V mutation in ZIKV NS2B (Figure S1C). Surprisingly, sequencing of ZDI-p10 revealed the presence of the same C1742U and A4338G changes, as well as an additional non-synonymous C2386U mutation that resulted in a T470M substitution in ZIKV E protein. Thus, the NS2B-I39V mutation is likely the candidate responsible for increased virulence of both ZN-p10 and ZDI-p10.

NS2B-I39V mutation confers the virulence of ZIKV in DENV2-immune mice

We next investigated whether the NS2B-I39V mutation shared by ZN-p10 and ZDI-p10 and/or the E-T470M mutation present only in ZDI-p10 were responsible for the enhanced pathogenicity observed in *Ifnar1*$^{-/-}$ mice. To address this, we engineered isogenic recombinant viruses (referred to as rZIKV strains) harboring NS2B-I39V or E-T470M from an infectious clone of ZIKV FSS13025 (Shan et al., 2016) (Figure S2A) and examined their virulence in DENV2-immune *Ifnar1*$^{-/-}$ mice, as described above. Notably, rZIKV-NS2B-I39V, but not rZIKV-E-T470M, exhibited enhanced virulence in DENV2-immune mice, as assessed by survival, weight loss, and clinical score (Figures 2A–2C). PWe also constructed rZIKV harboring both mutations to determine their potential additive/synergistic effects. Although we observed a small additive effect of NS2B-I39V and E-T470M substitutions that resulted in enhanced rZIKV disease development and accelerated mortality compared with NS2B-I39V alone in DENV2-immune mice, the effects were not significant (Figures 2A–2C). These results indicate that the NS2B-I39V mutation alone was sufficient to enable ZIKV to evade the protection conferred by pre-existing DENV immunity, increase replication, and enhance disease severity in *Ifnar1*$^{-/-}$ mice, whereas E-T470M had no effect, either alone or combined with NS2B-I39V.

NS2B-I39V mutation increases ZIKV maternal transmission and fetal mortality in pregnant mice and enhances ZIKV infection of human fetal NPCs

Congenital Zika syndrome can occur in infants born to ZIKV-infected mothers. Therefore, we investigated whether the ZIKV NS2B-I39V mutation affects placental transmission of ZIKV in DENV2-immune dams. For these experiments, female DENV2-immune *Ifnar1*$^{-/-}$ (C57BL/6 background) mice were mated with allogeneic (BALB/c) sires, and pregnant dams were infected IF with 10^4 FFU of rZIKV-WT or rZIKV-NS2B-I39V on embryonic

day 7.5 (E7.5). On E14.5, the fetuses, placenta, and decidua, and maternal serum, brain, and spleen were collected for analysis. As expected, most fetuses from rZIKV-WT-infected DENV2-immune dams were viable and only 3.5% of fetuses were resorbed (Figures 3A and 3B). In striking contrast, the vast majority (~90%) of fetuses from rZIKV-NS2B-I39V-infected dams were resorbed by E14.5 (Figures 3A–3C). Moreover, viral RNA levels were significantly higher in placenta/decidua, serum, brain, and spleen samples from dams infected with rZIKV-NS2B-I39V compared with rZIKV-WT (Figure 3D) and (Table S2). These results demonstrate that the NS2B-I39V mutation increased ZIKV infection in maternal tissues and markedly increased fetal resorption, suggesting a pathogenic role for the mutation during pregnancy. However, further investigation will be necessary to determine whether NS2B-I39V can enhance vertical transmission independently of the maternal viral load.

The ability of ZIKV to infect fetal NPCs plays a crucial role in the development of microcephaly (Dang et al., 2016; Garcez et al., 2016; Tang et al., 2016a). Therefore, we examined whether the NS2B-I39V mutation affects the infectivity of ZIKV in cultured human fetal NPCs. The cells were infected with rZIKV-WT or rZIKV-NS2B-I39V at a multiplicity of infection (MOI) of 0.1, and the culture supernatants were collected at 1 dpi and 3 dpi for quantification of ZIKV RNA by RT-qPCR and of infectious particles by FFA. At both time points examined, levels of viral RNA and numbers of infectious ZIKV particles were significantly higher in supernatants from NPCs infected with rZIKV-NS2B-I39V compared with rZIKV-WT (Figure 3D). These results indicate that the NS2B-I39V mutation increases ZIKV replication not only in pregnant and non-pregnant *Ifnar1*$^{-/-}$ mice but also in human NPCs.

The virulence of ZIKV in mice and infectivity in mosquitoes is enhanced by NS2B-I39V and the naturally occurring NS2B-I39T mutation

Given the enhanced replication and virulence of ZIKV NS2B-I39V in mice and its elevated infectivity in human NPCs, we next investigated whether this mutation was present in clinical ZIKV isolates circulating in the human population. We aligned the sequences of NS2B protein for all 1058 ZIKV clinical isolates currently available (as of September 1, 2021; ViPR database) and identified two isolates harboring an I39 mutation, both of which were I39T, from patients in Indonesia in 2017 and Japan in 2018 (GenBank AMK49492 and BBC70847, Figure S2B). We next examined the potential pathogenicity of this mutation by comparing DENV2-immune *Ifnar1*$^{-/-}$ mice infected with either rZIKV-NS2B-I39T or rZIKV-WT. Notably, rZIKV-NS2B-I39T-infected mice exhibited a transient increase in weight loss and a slightly more severe and sustained disease phenotype (score 3) compared with rZIKV-WT-infected mice (Figures 4A–4C). Nevertheless, all of the rZIKV-NS2B-I39T-infected animals survived to termination and the disease was much milder than that induced by rZIKV-NS2B-I39V (Figures 4A–4C). Thus, NS2B-I39T modestly enhances ZIKV pathogenicity in DENV2-immune mice compared with rZIKV-WT.

Screening of residue 39 in the NS2B proteins from all currently known isolates of ZIKV and related flaviviruses revealed that the predominant amino acids (>99% of isolates) at NS2B position 39 were Ile for ZIKV (n = 1058), DENV1 (n = 3648), and DENV3 (n = 1683); Thr

for DENV2 (n = 3023); Leu for DENV4 (n = 667); Met for YFV (n = 452); Phe for WNV (n = 267); and Ala for JEV (n = 387/387) (Table S3, Virus Pathogen Resource). These findings suggest that the ZIKV NS2B position 39 may be able to change from Ile to Leu, Met, Phe, or Ala, in addition to Val or Thr.

Finally, we examined whether the NS2B-I39V and NS2B-I39T mutations affected ZIKV infectivity in its natural vector, *A. aegypti.* We compared viral loads in *A. aegypti* (Rockefeller) mosquitoes after infection with rZIKV-WT, rZIKV-NS2B-I39V, or rZIKV-NS2B-I39T via a simulated sheep blood meal (Figure 4D). Mosquitoes were allowed to feed on the blood–virus mix for 30 min and then removed. Eight days later, viral genomic copy numbers in mosquitoes were measured by RT-qPCR analysis. The genomic copies (defined as $>10^4$ ZIKV genomic copies per mosquito; Figure 4E), were significantly increased on rZIKV-NS2B-I39V, or rZIKV-NS2B-I39T compared with rZIKV-WT. Furthermore, the absolute viral burdens (Figure 4F) were significantly (nearly 2-fold) higher for the two mutant rZIKV strains than for the rZIKV-WT strain, demonstrating that both mutations increased ZIKV infectivity in mosquitoes. Collectively, these results indicate that the induced and naturally occurring NS2B-I39 mutations significantly enhanced ZIKV fitness for transmission in its natural mosquito vector and increased pathogenicity in pregnant and non-pregnant mice the presence or absence of DENV2 immunity.

DISCUSSION

Since the explosive spread of ZIKV in the Americas in 2015–2016, one of the key challenges has been to understand the drivers of ZIKV evolution and exploit that knowledge to facilitate the prediction of future outbreaks. Viral RNA-dependent RNA polymerases exhibit high mutation rates and, given the mosquito–vertebrate transmission cycle, it seems inevitable that ZIKV outbreaks will continue to occur. In this regard, the spread of ZIKV into DENV-endemic regions has justifiably raised concerns about the impact of anti-DENV immunity on the evolutionary path of ZIKV. In the present study, we aimed to investigate these questions by simulating the natural transmission cycle of ZIKV in mosquitoes and DENV-endemic and -naive populations using cultured mosquito cells and DENV-naive or DENV2-immune *Ifnar1*$^{-/-}$ mice. This approach yielded several important results with implications for predicting future ZIKV outbreaks in both DENV-naive and -endemic regions. Of note, our results also suggest that the approach taken here could be a useful tool for the early identification of other flaviviral variants with enhanced infectivity/pathogenicity, and provide further evidence that viral infections in mice can be used to interrogate evolution of human-relevant arboviruses, in agreement with published studies (Johnson et al., 2020; Makhluf et al., 2013; Prestwood et al., 2008; Shresta et al., 2006).

In the present study, serial passaging of ZIKV induced the emergence of viral variants with only two non-synonymous mutations compared with the consensus genomic sequence of WT ZIKV, which is consistent with previous work demonstrating that DENV passaging between invertebrate and vertebrate host cells induces fewer mutations than does passaging through a single host cell line (Vasilakis et al., 2009). NS2B-I39V was present in ZIKV strains passaged in both DENV-naive and -immune mice, suggesting that pre-existing DENV immunity did not play a selective role. However, NS2B-I39V was sufficient to

not only enhance ZIKV virulence in naive mice but also to escape the protective effects of pre-existing DENV immunity, even during pregnancy, and to increase ZIKV infectivity of human NPCs, a critical host cell in humans. Additional support for the relevance of the I39 mutation came from the finding that a homologous substitution, NS2B-I39T, is present in circulating ZIKV isolates obtained in Asia in 2017 and 2018. Moreover, both NS2B-I39V and NS2B-I39T increased ZIKV infectivity and viral burden in mosquitoes after blood feeding, supporting the possibility that I39 represents a mutational hotspot with the potential to exacerbate disease transmission and severity not only in naive but also in DENV2-immune individuals in real-world settings. Thus, currently circulating ZIKV clinical isolates should be carefully monitored for the emergence of additional mutations at this position.

The clinical outcome of flavivirus infection is influenced by multiple virus and host interactions. Sequential infection by two different DENV serotypes or by ZIKV followed by DENV is known to be a major risk factor for severe dengue, in part due to the phenomenon of Ab-dependent enhancement of infection induced by pre-existing anti-flaviviral immunity (Halstead, 2007; Katzelnick et al., 2017, 2020; Salje et al., 2018). The robustness of the immune response elicited by prior DENV exposure can influence ZIKV infection outcome, through T cell-mediated cross-protection against ZIKV and antibody-mediated enhancement of ZIKV pathogenesis (Bardina et al., 2017; Chen et al., 2020; Gordon et al., 2019; Pedroso et al., 2019; Rathore et al., 2019; Regla-Nava et al., 2018; Rodriguez-Barraquer et al., 2019; Valentine et al., 2020; Wen et al., 2017a, 2017b, 2020). The present study reveals that ZIKV can readily adapt to enhance its virulence not only in a naive host but also in the presence of pre-existing cross-protective DENV immunity. This is in line with studies demonstrating that viral factors also influence DENV transmission and disease severity in endemic populations (Chan et al., 2019; Leitmeyer et al., 1999; Manokaran et al., 2015; OhAinle et al., 2011; Rodriguez-Roche et al., 2005). Based on these known patterns of DENV evolution and increased frequency of severe dengue disease over the past 60 years (Messina et al., 2019), it seems likely that ZIKV will continue to evolve in a manner that increases its virulence or transmission.

In conclusion, our study describes the use of a new approach to examine ZIKV evolution under various selective pressures by simulating the ZIKV–mosquito–vertebrate transmission cycle in DENV-naive and DENV-immune settings. We identified a ZIKV mutation in NS2B that had a profound effect on replication and/or pathogenicity in cultured mosquito and human cells, mosquitoes, and pregnant and non-pregnant mice. Moreover, we identified I39T as the only I39 mutation among >1000 clinical ZIKV isolates examined, and showed that this mutation significantly increased infectivity in human fetal NPCs and mosquitoes and modestly enhanced pathogenicity in mice. Thus, screening of natural isolates for changes in NS2B-I39 using the approach described here could be valuable for the early identification of ZIKV variants with greater infectivity and/or virulence, thus enabling concerted public health programs to be deployed to help avert an outbreak.

Limitations of the study

Our study has some limitations. We evaluated ZIKV virulence in *Ifnar1*$^{-/-}$ mice, and evaluated the impact of NS2B-I39V on infectivity of mosquito (C6/36) and nonhuman primate (Vero) cell lines, which are deficient in the RNA interference (Brackney et al., 2010) and type I IFN pathway (Emeny and Morgan, 1979), respectively. These mice and cell lines lacking key antiviral components may not faithfully model virus-host interactions. Therefore, testing pathogenicity in immunocompetent mice and infectivity in other cell types more relevant to the flavivirus–host relationship would be useful. Another limitation is that the transmissibility of the mutant ZIKV strains in the mosquito host needs to be investigated using a mosquito-mouse transmission model (Liu et al., 2017). Future studies also would be of interest to determine in which host and at which passaging cycle the NS2B-I39V mutation emerged. It would also be important to define the mechanism by which the I39V mutation alters ZIKV NS2B functions. NS2B serves as a cofactor for the viral NS2B–NS3 protease, which facilitates the cleavages of the ZIKV polyprotein into functional components, and additionally acts to promote the viral life cycle (Hill et al., 2018). As the central hydrophilic domain (residues 44–96) but not the hydrophobic regions (residues 1–44 and 97–125) of NS2B is required for the protease activity of NS3 (Lei et al., 2016; Phoo et al., 2016; Zhang et al., 2016), the I39V substitution is likely to impact assembly and functions of viral replication complex components other than activation of the NS3 protease.

STAR★METHODS

RESOURCE AVAILABILITY

Lead contact—Further information and requests for resources and reagents should be directed to and will be fulfilled by the lead contact, Sujan Shresta (sujan@lji.org).

Materials availability—This study did not generate new unique reagents.

Data and code availability

- All data supporting the findings of this study are available within the paper and its supplemental information files.
- This study did not generate any unique datasets or code.
- Any additional information required to reanalyze the data reported in this paper is available from the lead contact upon request.

EXPERIMENTAL MODEL AND SUBJECT DETAILS

Animals—*Ifnar1*$^{-/-}$ mice (C57BL/6 background) were bred in a specific pathogen-free facility at La Jolla Institute for Immunology (Yauch et al., 2009). *Ifnar1*$^{-/-}$ females o males were challenged at 4- to 5-weeks of age for not pregnant studies. For model ZIKV pregnancy infection female mice were mated at 8–10 weeks of age. This study followed the guidelines approved by the Institutional Animal Care and Use Committee of La Jolla Institute for Immunology (protocol #AP028–221-0615).

Cell lines—C6/36 mosquito cells were grown in Leibovitz's L-15 (Thermo Fisher Scientific, cat. #11415064) supplemented with 10% fetal bovine serum (FBS) (Thermo Fisher Scientific, cat. #16000044), 1% penicillin/streptomycin (Thermo Fisher Scientific cat. #15140–122), and 1% HEPES (Thermo Fisher Scientific, cat. #15630080) at 28°C. BHK-21 cells were grown in MEM α (Fisher, cat. #12–561-072) supplemented with 10% FBS, 1% penicillin/streptomycin, and 1% HEPES at 37°C in a 5% CO_2 atmosphere. Vero cells were purchased from ATCC (CRL-1586) and maintained in high-glucose Dulbecco's modified Eagle's medium supplemented with 10% fetal bovine serum (FBS) (HyClone Laboratories, South Logan, UT), 1% HEPES, and 1% penicillin/streptomycin at 37°C in a 5% CO_2 atmosphere. Human fetal neural progenitor cells (NPCs) were kindly provided by A. V Terskikh (Sanford Burnham Prebys Medical Discovery Institute, La Jolla, USA) and were maintained in DMEM/F12, (Corning, 10–092-CV), 1X N-2 supplement (Thermo Fisher Scientific, 17502048), 1X B-27™ without vitamin A (Thermo Fisher Scientific, 12587010), 20 ng/mL human FGF-basic (Thermo Fisher Scientific, PHG0263), 1X MEM non-essential amino acids solution (Thermo Fisher Scientific, 11140050), and 1X Penicillin-Streptomycin (Thermo Fisher Scientific, 15140122) on PLO/laminin-coated plates at 37°C in a 5% CO_2 atmosphere. Cells were passaged using StemPro™ Accutase™ Cell Dissociation Reagent (Thermo Fisher Scientific, A1110501) as needed.

Viruses—ZIKV Asian lineage strain FSS13025 (Cambodia, 2010) was obtained from the World Reference Center for Emerging Viruses and Arboviruses (Galveston, TX). The mouse-adapted DENV2 strain S221 is a biological clone derived from DENV2 D2S1O (Shresta et al., 2006; Yauch et al., 2009). ZIKV and DENV2 were propagated in C6/36 Aedes albopictus cells (American Type Culture Collection [ATCC], CRL-1660).

METHOD DETAILS

Infectious virus and viral RNA quantification—Viral titers were measured using a focus-forming assay (FFA) with baby hamster kidney (BHK)-21 cells (ATCC, CCL-10) or by RT-qPCR analysis (Elong Ngono et al., 2017), using the QuantaBio qScript one-step qRT-PCR kit (VWR, cat. #101414–172) and probes and primers described in the key resources table.

DENV2 and ZIKV infection of mice—To establish DENV immunity, 5-week-old female *Ifnar1*$^{-/-}$ mice were inoculated *via* intraperitoneal (IP) injection with 10^3 FFU of DENV2 S221. At 8–10 weeks of age, groups of naive and DENV2-immune mice (30 dpi) were infected with vehicle (PBS/10% FBS) or with 10^4 FFU of WT ZIKV, ZN-p10, ZDI-p10, rZIKV-WT, rZIKV-NS2B-I39V or rZIKV-NS2B-I39T in vehicle (PBS/10% FBS) via intra-footpad (IF, 20 μL) injection. Mice that lost >20% of their body weight were euthanized.

For experiments with pregnant mice, DENV2-immune *Ifnar1*$^{-/-}$ dams were mated with BALB/c males and checked daily for the appearance of vaginal plugs. The day of vaginal plug appearance was defined as embryonic day 0.5 (E0.5). On E7.5, dams were infected IF with 10^4 FFU of rZIKV-WT or rZIKV-NS2B-I39V. On E14.5, dams were euthanized, blood was collected by cardiac puncture, and fetuses and maternal tissues were harvested for analysis.

Disease scoring—Mice were monitored daily for weight and clinical scores from day 0 to day 15 dpi. Clinical scores ranged from 1 – 7: 1, heathy mice with a smooth coat and bright, alert eyes; 2, mice are slightly ruffled around the head and neck, but active and alert; 3, mice have a ruffled coat throughout the body, but still active and alert; 4, mice have a very ruffled coat and slightly closed eyes, they walk slowly, and they have mild lethargy; 5, mice have a very ruffled coat and closed inset eyes, slow to no movement but will return to the upright position if put on the side; 6, mice have a very ruffled coat and closed inset eyes, are moribund, they have no movement or uncontrollable spastic movements, will not return to upright position if put on its side, and completely unaware or in noticeable distress and require humane euthanasia; 7, mice are deceased. Mice were humanely euthanized if weight loss was greater than or equal to 20% of their body mass or if their clinical score was a 6.

Virus passaging and sequencing—Groups of 3 naive and 3 DENV2 immune *Ifnar1*$^{-/-}$ mice were inoculated intravenously (IV, retro-orbital injection, 100 μL) with 10^4 FFU of ZIKV to generate ZIKV strains designated ZN-p10 and ZDI-p10 ZIKV, respectively. On day 3 dpi, the mice were euthanized using CO_2 and cervical dislocation, whole blood was collected via cardiac puncture, and sera were prepared and pooled for each group of 3. Virus in the sera were amplified in C6/36 cells for 7–10 days. The supernatants were then harvested and clarified, and 200 μL of untitered supernatant (i.e., blind passaging) was injected IV into a second set of naive mice or DENV2-immune *Ifnar1*$^{-/-}$ mice (n = 3). This entire cycle was repeated 10 times to obtain the final ZN-p10 and ZDI-p10 stocks.

For nucleotide sequence analysis, viral RNA was isolated using an RNeasy Mini Kit (Qiagen). ZIKV sequencing libraries were constructed using the NEBNext® Ultra II™ Directional RNA Library Prep Kit for Illumina® (New England BioLabs, Ipswich, MA). Libraries were sequenced on the Illumina NextSeq 500 and data were processed in BaseSpace (basespace.illumina.com). Reads were aligned to the ZIKV FSS13025 (2010 Cambodian isolate) sequence from GenBank (KU955593.1) and aligned with BWA using default settings. Variants were called with the Pisces Variant Caller (https://github.com/Illumina/Pisces). A frequency change of >90% was considered a major mutation.

Focus-forming assay—The FFA was performed with BHK-21 cells as described (Elong Ngono et al., 2017). Mouse organs were homogenized in 1 mL MEM medium for 3 min using a TissueLyser II (Qiagen) and centrifuged for 1 min at 6000 g. Aliquots of homogenate supernatants or sera (100 μL) were diluted serially, added to BHK-21 cells (n=2), and incubated at 37°C for 1 h. The supernatant was then aspirated, and the cells were overlaid with 1% carboxymethyl cellulose (CMC) medium and incubated for 2.5 days. The cells were fixed with 4% formalin (Fisher), permeabilized with 1% Triton X-100, blocked with PBS/10% FBS solution, and incubated with the pan flavivirus-specific mAb 4G2 (1 μg/mL) for 1 h at room temperature. The cells were washed and incubated with horseradish peroxidase-conjugated goat anti-mouse IgG (1:1000). Foci were developed using True Blue substrate and counted manually.

Viral RNA quantification by RT-qPCR—Viral RNA was extracted from mouse serum and tissue samples using a QIAmp Viral RNA Mini Kit (Qiagen) and an RNeasy Mini Kit (Qiagen), respectively. RT-qPCR was performed using a qScript One-Step RT-qPCR

Kit (Quanta Bioscience) with a CFX96 Touch Real-Time PCR detection system (Bio-Rad, CFX Manager 3.1). ZIKV-specific primers have been described (Tang et al., 2016b). Cycling conditions were 45°C for 15 min, 95°C for 15 min, followed by 40 cycles of 95°C for 15 s and 60°C for 15 s, and a final extension of 72°C for 30 min. Viral RNA concentration was calculated using a standard curve composed of four 100-fold serial dilutions of *in vitro*-transcribed RNA from ZIKV strain FSS13025.

Plasmid construction—E-T470M, NS2B-I39V, E-T470M + NS2B-I39V, and NS2B-I39T mutations were introduced into ZIKV cDNA infectious clone pFLZIKV (Shan et al., 2016). Overlap PCR containing the mutation was performed to amplify the DNA fragment between unique restriction sites AvrII, SphI, and NaeI (New England BioLabs, Ipswich, MA) (Shan et al., 2017). Full-length plasmids were verified by DNA sequencing. All primers are listed in Table S1.

***In vitro* RNA transcription and transfection—**Full-genome rZIKV-WT, rZIKV-E-T470M, rZIKV-NS2B-I39V, rZIKV-NS2B-I39T and rZIKV-E-T470M + NS2B-I39V RNAs were *in vitro* transcribed from cDNA plasmids pre-linearized with ClaI using a T7 mMessage mMachine kit (Ambion, Austin, TX). Transcribed RNA was precipitated with lithium chloride, washed with 70% ethanol, resuspended in RNase-free water, quantified by spectrophotometry, and stored at −80°C in aliquots. RNA transcripts (10 μg) were electroporated into Vero cells following a protocol described previously (Shan et al., 2016).

Infection of mosquitoes with recombinant ZIKV—*Aedes aegypti* Rockefeller strain mosquitoes were maintained in an illuminated incubator (Model 818, Thermo Fisher Scientific) under standard conditions of 28°C, 80% humidity, and a 12-h light/dark cycle. For membrane blood-feeding experiments, complement-inactivated sheep blood (C26218, Hemostat laboratories) was mixed with Vero cell culture supernatant containing the WT or mutant ZIKV strains (10^6 PFU/mL) and the virus-blood mixture was loaded into the reservoir of a Hemotek system (5W1, Hemotek). Seven-day-old starved female mosquitoes were added and allowed to feed for 30 min in the dark. The fully engorged mosquitoes were then removed, reared for 8 days, and analyzed by RT-qPCR.

QUANTIFICATION AND STATISTICAL ANALYSIS

Statistics and graphs—All data were analyzed with Prism software, version 8.0 (GraphPad Software). Data are presented as the mean ± SEM. The Gehan–Breslow–Wilcoxon test was used to analyze survival and two-tailed Mann–Whitney and Fisher's exact tests were used for all other group mean comparisons. $p < 0.05$ was considered statistically significant.

Supplementary Material

Refer to Web version on PubMed Central for supplementary material.

ACKNOWLEDGMENTS

This study was supported by grants from the National Institutes of Health (R01 AI153500, R01 AI163188, R56 AI148635, and U01 AI151810 to S.S.; R01 NS106387 to J.G.G.; R01 AI134907, R43 AI145617, and UL1 TR001439 to P.-Y.S.) and from the Sealy & Smith Foundation, the Kleberg Foundation, the John S. Dunn Foundation, the Amon G. Carter Foundation, the Gilson Longenbaugh Foundation, and the Summerfield Robert Foundation to P.-Y.S.

REFERENCES

Bardina SV, Bunduc P, Tripathi S, Duehr J, Frere JJ, Brown JA, Nachbagauer R, Foster GA, Krysztof D, Tortorella D, et al. (2017). Enhancement of Zika virus pathogenesis by preexisting antiflavivirus immunity. Science 356, 175–180. [PubMed: 28360135]

Besnard M, Lastere S, Teissier A, Cao-Lormeau V, and Musso D (2014). Evidence of perinatal transmission of Zika virus, French Polynesia, December 2013 and February 2014. Euro Surveill. 19, 20751. [PubMed: 24721538]

Bhatt S, Gething PW, Brady OJ, Messina JP, Farlow AW, Moyes CL, Drake JM, Brownstein JS, Hoen AG, Sankoh O, et al. (2013). The global distribution and burden of dengue. Nature 496, 504–507. [PubMed: 23563266]

Brackney DE, Scott JC, Sagawa F, Woodward JE, Miller NA, Schilkey FD, Mudge J, Wilusz J, Olson KE, Blair CD, et al. (2010). C6/36 Aedes albopictus cells have a dysfunctional antiviral RNA interference response. PLoS Negl. Trop. Dis. 4, e856. [PubMed: 21049065]

Chan KWK, Watanabe S, Jin JY, Pompon J, Teng D, Alonso S, Vijaykrishna D, Halstead SB, Marzinek JK, Bond PJ, et al. (2019). A T164S mutation in the dengue virus NS1 protein is associated with greater disease severity in mice. Sci. Transl. Med. 11.

Chen D, Duan Z, Zhou W, Zou W, Jin S, Li D, Chen X, Zhou Y, Yang L, Zhang Y, et al. (2020). Japanese encephalitis virus-primed CD8+ T cells prevent antibody-dependent enhancement of Zika virus pathogenesis. J. Exp. Med. 217, e20192152. [PubMed: 32501510]

Dang J, Tiwari SK, Lichinchi G, Qin Y, Patil VS, Eroshkin AM, and Rana TM (2016). Zika virus depletes neural progenitors in human cerebral organoids through activation of the innate immune receptor TLR3. Cell Stem Cell 19, 258–265. [PubMed: 27162029]

Elong Ngono A, and Shresta S (2018). Immune response to dengue and Zika. Annu. Rev. Immunol. 36, 279–308. [PubMed: 29345964]

Elong Ngono A, and Shresta S (2019). Cross-reactive T cell immunity to dengue and Zika viruses: new insights into vaccine development. Front. Immunol. 10, 1316. [PubMed: 31244855]

Elong Ngono A, Vizcarra EA, Tang WW, Sheets N, Joo Y, Kim K, Gorman MJ, Diamond MS, and Shresta S (2017). Mapping and role of the CD8+ T cell response during primary Zika virus infection in mice. Cell Host Microbe 21, 35–46. [PubMed: 28081442]

Emeny JM, and Morgan MJ (1979). Regulation of the interferon system: evidence that Vero cells have a genetic defect in interferon production. J. Gen. Virol. 43, 247–252. [PubMed: 113494]

Faria NR, Quick J, Claro IM, Theze J, de Jesus JG, Giovanetti M, Kraemer MUG, Hill SC, Black A, da Costa AC, et al. (2017). Establishment and cryptic transmission of Zika virus in Brazil and the Americas. Nature 546, 406–410. [PubMed: 28538727]

Garcez PP, Loiola EC, Madeiro da Costa R, Higa LM, Trindade P, Delvecchio R, Nascimento JM, Brindeiro R, Tanuri A, and Rehen SK (2016). Zika virus impairs growth in human neurospheres and brain organoids. Science 352, 816–818. [PubMed: 27064148]

Gordon A, Gresh L, Ojeda S, Katzelnick LC, Sanchez N, Mercado JC, Chowell G, Lopez B, Elizondo D, Coloma J, et al. (2019). Prior dengue virus infection and risk of Zika: a pediatric cohort in Nicaragua. PLoS Med. 16, e1002726. [PubMed: 30668565]

Halstead SB (2007). Dengue. Lancet 370, 1644–1652. [PubMed: 17993365]

Hill ME, Kumar A, Wells JA, Hobman TC, Julien O, and Hardy JA (2018). The unique cofactor region of Zika virus NS2B-NS3 protease facilitates cleavage of key host proteins. ACS Chem. Biol. 13, 2398–2405.

Johnson KEE, Noval MG, Rangel MV, De Jesus E, Geber A, Schuster S, Cadwell K, Ghedin E, and Stapleford KA (2020). Mapping the evolutionary landscape of Zika virus infection in immunocompromised mice. Virus Evol. 6, veaa092. [PubMed: 33408879]

Katzelnick LC, Gresh L, Halloran ME, Mercado JC, Kuan G, Gordon A, Balmaseda A, and Harris E (2017). Antibody-dependent enhancement of severe dengue disease in humans. Science 358, 929–932. [PubMed: 29097492]

Katzelnick LC, Narvaez C, Arguello S, Lopez Mercado B, Collado D, Ampie O, Elizondo D, Miranda T, Bustos Carillo F, Mercado JC, et al. (2020). Zika virus infection enhances future risk of severe dengue disease. Science 369, 1123–1128. [PubMed: 32855339]

Lazear HM, and Diamond MS (2016). Zika virus: new clinical syndromes and its emergence in the western hemisphere. J. Virol. 90, 4864–4875. [PubMed: 26962217]

Lei J, Hansen G, Nitsche C, Klein CD, Zhang L, and Hilgenfeld R (2016). Crystal structure of Zika virus NS2B-NS3 protease in complex with a boronate inhibitor. Science 353, 503–505. [PubMed: 27386922]

Leitmeyer KC, Vaughn DW, Watts DM, Salas R, Villalobos I, de C, Ramos C, and Rico-Hesse R (1999). Dengue virus structural differences that correlate with pathogenesis. J. Virol. 73, 4738–4747. [PubMed: 10233934]

Liu Y, Liu J, Du S, Shan C, Nie K, Zhang R, Li XF, Zhang R, Wang T, Qin CF, et al. (2017). Evolutionary enhancement of Zika virus infectivity in Aedes aegypti mosquitoes. Nature 545, 482–486. [PubMed: 28514450]

Major CG, Paz-Bailey G, Hills SL, Rodriguez DM, Biggerstaff BJ, and Johansson M (2021). Risk estimation of sexual transmission of Zika virus-United States, 2016–2017. J Infect Dis.

Makhluf H, Buck MD, King K, Perry ST, Henn MR, and Shresta S (2013). Tracking the evolution of dengue virus strains D2S10 and D2S20 by 454 pyrosequencing. PLoS One 8, e54220. [PubMed: 23342105]

Manokaran G, Finol E, Wang C, Gunaratne J, Bahl J, Ong EZ, Tan HC, Sessions OM, Ward AM, Gubler DJ, et al. (2015). Dengue subgenomic RNA binds TRIM25 to inhibit interferon expression for epidemiological fitness. Science 350, 217–221. [PubMed: 26138103]

Mansuy JM, Suberbielle E, Chapuy-Regaud S, Mengelle C, Bujan L, Marchou B, Delobel P, Gonzalez-Dunia D, Malnou CE, Izopet J, et al. (2016). Zika virus in semen and spermatozoa. Lancet Infect. Dis. 16, 1106–1107. [PubMed: 27676340]

Messina JP, Brady OJ, Golding N, Kraemer MUG, Wint GRW, Ray SE, Pigott DM, Shearer FM, Johnson K, Earl L, et al. (2019). The current and future global distribution and population at risk of dengue. Nat. Microbiol. 4, 1508–1515. [PubMed: 31182801]

Musso D, and Gubler DJ (2016). Zika virus. Clin. Microbiol. Rev. 29, 487–524. [PubMed: 27029595]

OhAinle M, Balmaseda A, Macalalad AR, Tellez Y, Zody MC, Saborio S, Nunez A, Lennon NJ, Birren BW, Gordon A, et al. (2011). Dynamics of dengue disease severity determined by the interplay between viral genetics and serotype-specific immunity. Sci. Transl. Med. 3, 114ra128.

Pedroso C, Fischer C, Feldmann M, Sarno M, Luz E, Moreira-Soto A, Cabral R, Netto EM, Brites C, Kummerer BM, et al. (2019). Cross-protection of dengue virus infection against congenital zika syndrome, northeastern Brazil. Emerg. Infect. Dis. 25, 1485–1493. [PubMed: 31075077]

Peixoto HM, Romero GAS, de Araujo WN, and de Oliveira MRF (2019). Guillain-Barre syndrome associated with Zika virus infection in Brazil: a cost-of-illness study. Trans. R. Soc. Trop. Med. Hyg. 113, 252–258. [PubMed: 30892628]

Phoo WW, Li Y, Zhang Z, Lee MY, Loh YR, Tan YB, Ng EY, Lescar J, Kang C, and Luo D (2016). Structure of the NS2B-NS3 protease from Zika virus after self-cleavage. Nat. Commun. 7, 13410. [PubMed: 27845325]

Pierson TC, and Diamond MS (2020). The continued threat of emerging flaviviruses. Nat. Microbiol. 5, 796–812. [PubMed: 32367055]

Prestwood TR, Prigozhin DM, Sharar KL, Zellweger RM, and Shresta S (2008). A mouse-passaged dengue virus strain with reduced affinity for heparan sulfate causes severe disease in mice by establishing increased systemic viral loads. J. Virol. 82, 8411–8421. [PubMed: 18562532]

Rasmussen SA, Jamieson DJ, Honein MA, and Petersen LR (2016). Zika virus and birth defects–reviewing the evidence for causality. N. Engl. J. Med. 374, 1981–1987. [PubMed: 27074377]

Rathore APS, Saron WAA, Lim T, Jahan N, and St John AL (2019). Maternal immunity and antibodies to dengue virus promote infection and Zika virus-induced microcephaly in fetuses. Sci. Adv. 5, eaav3208. [PubMed: 30820456]

Regla-Nava JA, Elong Ngono A, Viramontes KM, Huynh AT, Wang YT, Nguyen AT, Salgado R, Mamidi A, Kim K, Diamond MS, et al. (2018). Cross-reactive Dengue virus-specific CD8(+) T cells protect against Zika virus during pregnancy. Nat. Commun. 9, 3042. [PubMed: 30072692]

Rico-Mendoza A, Alexandra PR, Chang A, Encinales L, and Lynch R (2019). Co-circulation of dengue, chikungunya, and Zika viruses in Colombia from 2008 to 2018. Rev. Panam Salud Publica 43, e49. [PubMed: 31171921]

Rodriguez-Barraquer I, Costa F, Nascimento EJM, Nery NJ, Castanha PMS, Sacramento GA, Cruz J, Carvalho M, De Olivera D, Hagan JE, et al. (2019). Impact of preexisting dengue immunity on Zika virus emergence in a dengue endemic region. Science 363, 607–610. [PubMed: 30733412]

Rodriguez-Morales AJ, Villamil-Gomez WE, and Franco-Paredes C (2016). The arboviral burden of disease caused by co-circulation and co-infection of dengue, chikungunya and Zika in the Americas. Trav. Med. Infect. Dis. 14, 177–179.

Rodriguez-Roche R, Alvarez M, Gritsun T, Halstead S, Kouri G, Gould EA, and Guzman MG (2005). Virus evolution during a severe dengue epidemic in Cuba, 1997. Virology 334, 154–159. [PubMed: 15780865]

Salje H, Cummings DAT, Rodriguez-Barraquer I, Katzelnick LC, Lessler J, Klungthong C, Thaisomboonsuk B, Nisalak A, Weg A, Ellison D, et al. (2018). Reconstruction of antibody dynamics and infection histories to evaluate dengue risk. Nature 557, 719–723. [PubMed: 29795354]

Shan C, Muruato AE, Nunes BTD, Luo H, Xie X, Medeiros DBA, Wakamiya M, Tesh RB, Barrett AD, Wang T, et al. (2017). A live-attenuated Zika virus vaccine candidate induces sterilizing immunity in mouse models. Nat. Med. 23, 763–767. [PubMed: 28394328]

Shan C, Xia H, Haller SL, Azar SR, Liu Y, Liu J, Muruato AE, Chen R, Rossi SL, Wakamiya M, et al. (2020). A Zika virus envelope mutation preceding the 2015 epidemic enhances virulence and fitness for transmission. Proc. Natl. Acad. Sci. U S A. 117, 20190–20197. [PubMed: 32747564]

Shan C, Xie X, Muruato AE, Rossi SL, Roundy CM, Azar SR, Yang Y, Tesh RB, Bourne N, Barrett AD, et al. (2016). An infectious cDNA clone of Zika virus to study viral virulence, mosquito transmission, and antiviral inhibitors. Cell Host Microbe 19, 891–900. [PubMed: 27198478]

Shresta S, Sharar KL, Prigozhin DM, Beatty PR, and Harris E (2006). Murine model for dengue virus-induced lethal disease with increased vascular permeability. J. Virol. 80, 10208–10217. [PubMed: 17005698]

Tang H, Hammack C, Ogden SC, Wen Z, Qian X, Li Y, Yao B, Shin J, Zhang F, Lee EM, et al. (2016a). Zika virus infects human cortical neural progenitors and attenuates their growth. Cell Stem Cell 18, 587–590. [PubMed: 26952870]

Tang WW, Young MP, Mamidi A, Regla-Nava JA, Kim K, and Shresta S (2016b). A mouse model of Zika virus sexual transmission and vaginal viral replication. Cell Rep. 17, 3091–3098. [PubMed: 28009279]

Valentine KM, Croft M, and Shresta S (2020). Protection against dengue virus requires a sustained balance of antibody and T cell responses. Curr. Opin. Virol. 43, 22–27. [PubMed: 32798886]

Vasilakis N, Deardorff ER, Kenney JL, Rossi SL, Hanley KA, and Weaver SC (2009). Mosquitoes put the brake on arbovirus evolution: experimental evolution reveals slower mutation accumulation in mosquito than vertebrate cells. PLoS Pathog. 5, e1000467. [PubMed: 19503824]

Wen J, Elong Ngono A, Angel Regla-Nava J, Kim K, Gorman MJ, Diamond MS, and Shresta S (2017a). Dengue virus-reactive CD8+ T cells mediate cross-protection against subsequent Zika virus challenge. Nat. Commun. 8, 1459. [PubMed: 29129917]

Wen J, and Shresta S (2019). Antigenic cross-reactivity between Zika and dengue viruses: is it time to develop a universal vaccine? Curr. Opin. Immunol. 59, 1–8. [PubMed: 30884384]

Wen J, Tang WW, Sheets N, Ellison J, Sette A, Kim K, and Shresta S (2017b). Identification of Zika virus epitopes reveals immunodominant and protective roles for dengue virus cross-reactive CD8+ T cells. Nat. Microbiol. 2, 17036. [PubMed: 28288094]

Wen J, Wang YT, Valentine KM, Dos Santos Alves RP, Xu Z, Regla-Nava JA, Ngono AE, Young MP, Ferreira LCS, and Shresta S (2020). CD4(+) T cells cross-reactive with dengue and Zika viruses protect against Zika virus infection. Cell Rep. 31, 107566. [PubMed: 32348763]

Xia H, Luo H, Shan C, Muruato AE, Nunes BTD, Medeiros DBA, Zou J, Xie X, Giraldo MI, Vasconcelos PFC, et al. (2018). An evolutionary NS1 mutation enhances Zika virus evasion of host interferon induction. Nat. Commun. 9, 414. [PubMed: 29379028]

Yauch LE, Zellweger RM, Kotturi MF, Qutubuddin A, Sidney J, Peters B, Prestwood TR, Sette A, and Shresta S (2009). A protective role for dengue virus-specific CD8+ T cells. J. Immunol. 182, 4865–4873. [PubMed: 19342665]

Yuan L, Huang XY, Liu ZY, Zhang F, Zhu XL, Yu JY, Ji X, Xu YP, Li G, Li C, et al. (2017). A single mutation in the prM protein of Zika virus contributes to fetal microcephaly. Science 358, 933–936. [PubMed: 28971967]

Zhang Z, Li Y, Loh YR, Phoo WW, Hung AW, Kang C, and Luo D (2016). Crystal structure of unlinked NS2B-NS3 protease from Zika virus. Science 354, 1597–1600. [PubMed: 27940580]

Highlights

- ZIKV virus evolution increases pathogenesis in mice
- I39V mutation in the NS2B protein confers escape from preexisting DENV immunity
- I39V or I39T mutation increases ZIKV replication in NPCs and mosquitoes

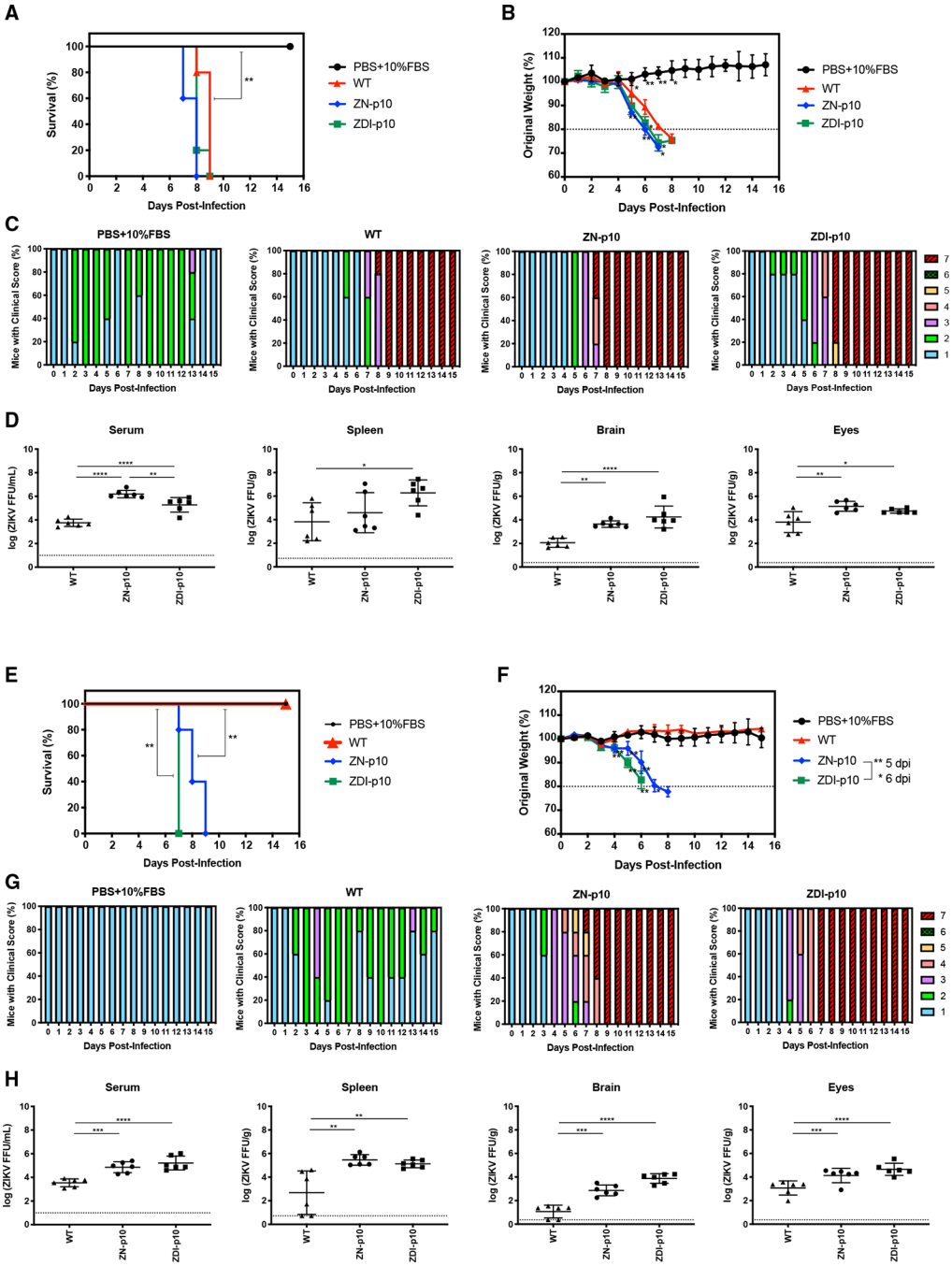

Figure 1. Clinical phenotype and viral replication in naive and DENV-immune *Ifnar1*$^{-/-}$ mice inoculated with passaged ZIKV strains

(A–D, B, and F) DENV2-immune *Ifnar1*$^{-/-}$ mice were generated by intraperitoneal injection of 10^3 FFU DENV2 S221. Thirty days later, groups of naive (A–D) and DENV2-immune (E–H) *Ifnar1*$^{-/-}$ mice (n = 5) were injected intra-footpad with PBS/10% FBS or 10^4 FFU of unpassaged ZIKV FSS13025 (WT) or ZIKV passaged for 10 cycles through mosquito cells and naive (ZN-p10) or DENV2-immune (ZDI-p10) *Ifnar1*$^{-/-}$ mice. Animals were monitored daily for survival (A and E), weight loss (B and F), and clinical score (C and G). Animals that lost >20% of their initial body weight were euthanized.

(D and H) Parallel groups of mice were euthanized 3 days after ZIKV infection, and infectious ZIKV levels in serum and the indicated organs were quantified by FFA (n = 6/group). Data are presented as the mean ± SEM and were pooled from two independent experiments. *p < 0.05, **p < 0.01, ***p < 0.001, ****p < 0.0001 by the Gehan–Breslow–Wilcoxon test (survival) and the two-tailed Mann–Whitney test (body weights and viral titers).

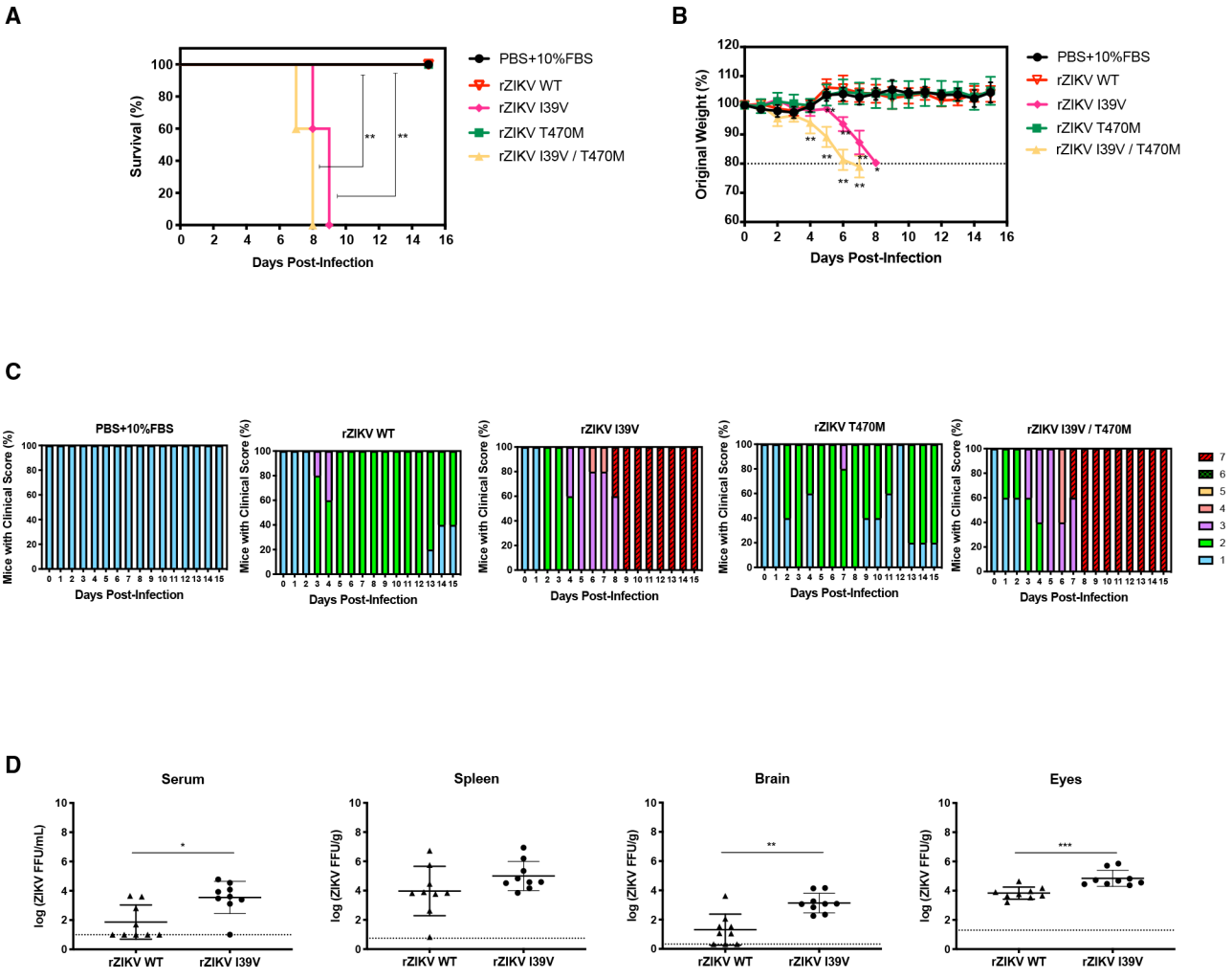

Figure 2. Clinical phenotype and viral replication in DENV-immune *Ifnar1*$^{-/-}$ mice inoculated with recombinant mutant ZIKV strains

(A–D) DENV2-immune *Ifnar1*$^{-/-}$ mice were generated by intraperitoneal injection of 10^3 FFU DENV2 S221. Thirty days later, groups of DENV2-immune *Ifnar1*$^{-/-}$ mice (n = 5) were injected intra-footpad with PBS/10% FBS or 10^4 FFU of recombinant ZIKV harboring the indicated mutations. Animals were monitored daily for survival (A), weight loss (B), and clinical score (C). Animals that lost >20% of their initial body weight were euthanized. (D) Parallel groups of mice were euthanized 3 days after ZIKV infection, and levels of infectious ZIKV in serum and the indicated organs were quantified (n = 9/group). Data are presented as the mean ± SEM and were pooled from two independent experiments. *p < 0.05, **p < 0.01, ***p < 0.001 by the Gehan–Breslow–Wilcoxon test (survival) or two-tailed Mann–Whitney test (body weights and viral titers).

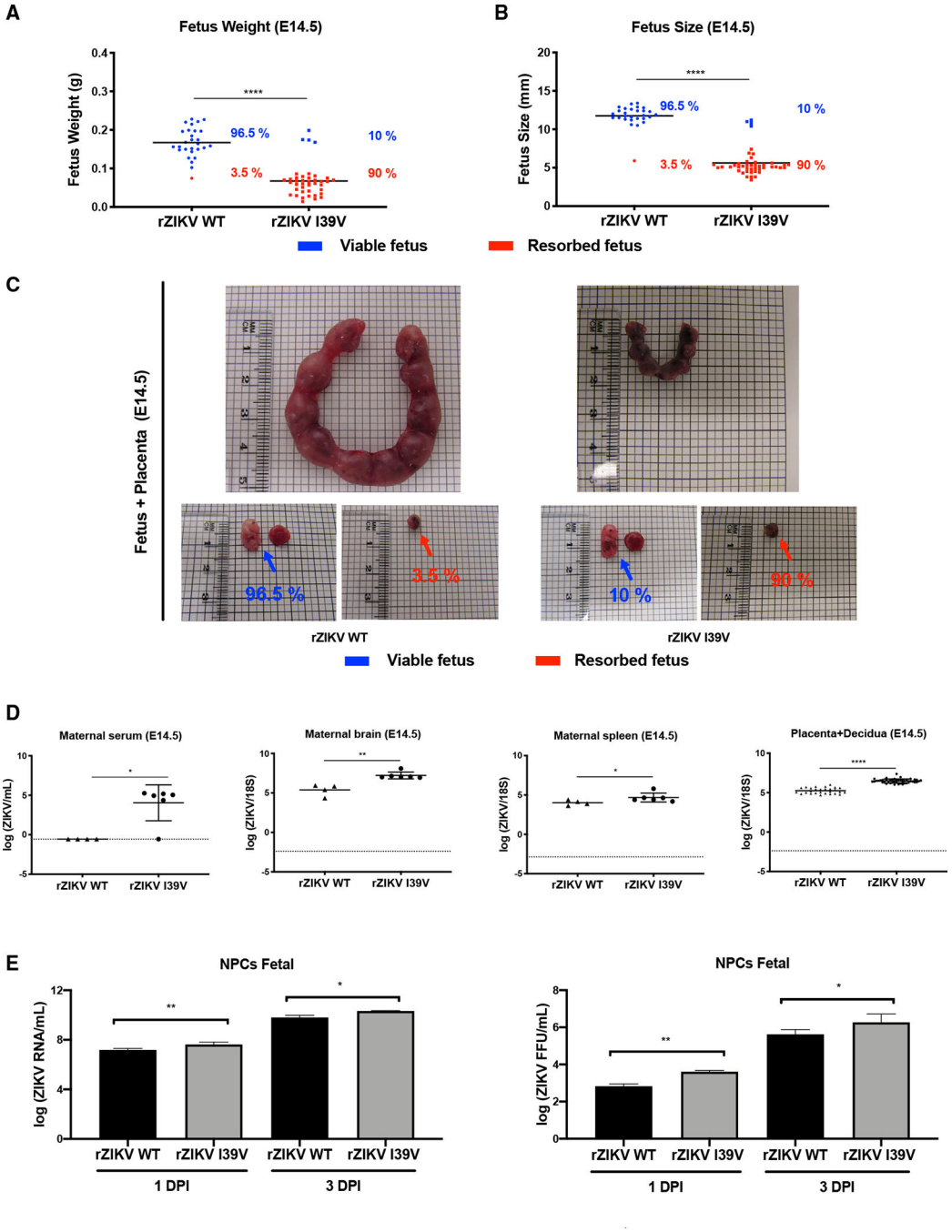

Figure 3. ZIKV I39V mutation increases placental transmission in DENV2-immune *Ifnar1*$^{-/-}$ mice and infectivity in human fetal neural progenitor cells

DENV2-immune *Ifnar1*$^{-/-}$ mice were generated by intraperitoneal injection of 10^3 FFU DENV2 S221 for 30 days, and DENV-immune dams were then mated with BALB/c sires. On embryonic day 7.5 (E7.5), pregnant mice were injected intra-footpad with 10^4 FFU of recombinant wild-type ZIKV (rZIKV-WT) or rZIKV-NS2B-I39V. On E14.5, the mice were euthanized, and fetuses and maternal tissues were harvested for analysis.

(A and B) Body weights (A) and body length (B) of fetuses on E14.5. Blue and red symbols represent viable and resorbed fetuses, respectively.

(C) Representative placenta and fetuses from dams in each mouse group. Blue and red arrows indicate viable and resorbed fetuses, respectively.
(D) RT-qPCR analysis of ZIKV RNA levels in maternal serum, brain, spleen, and placenta/decidua on E14.5. Data are presented as the mean ± SEM and were pooled from independent experiments with a total of 28 fetuses from four mothers for the rZIKV-WT group and 40 fetuses from six mothers for the rZIKV-NS2B-I39V group.
(E) Kinetics of rZIKV-WT and rZIKV-NS2B-I39V replication in human fetal NPCs. Human fetal NPCs were infected with the indicated viruses at an MOI of 1. RT-qPCR and FFA were performed on days 1 and 3 post-infection (1 dpi and 3 dpi) to measure levels of ZIKV RNA and infectious virus in culture supernatants, respectively. Data are presented as the mean ± SEM of triplicates and represent pooled results from three independent experiments with cells derived from three donors. *$p < 0.05$, **$p < 0.01$, ****$p < 0.0001$ by the two-tailed Mann–Whitney test.

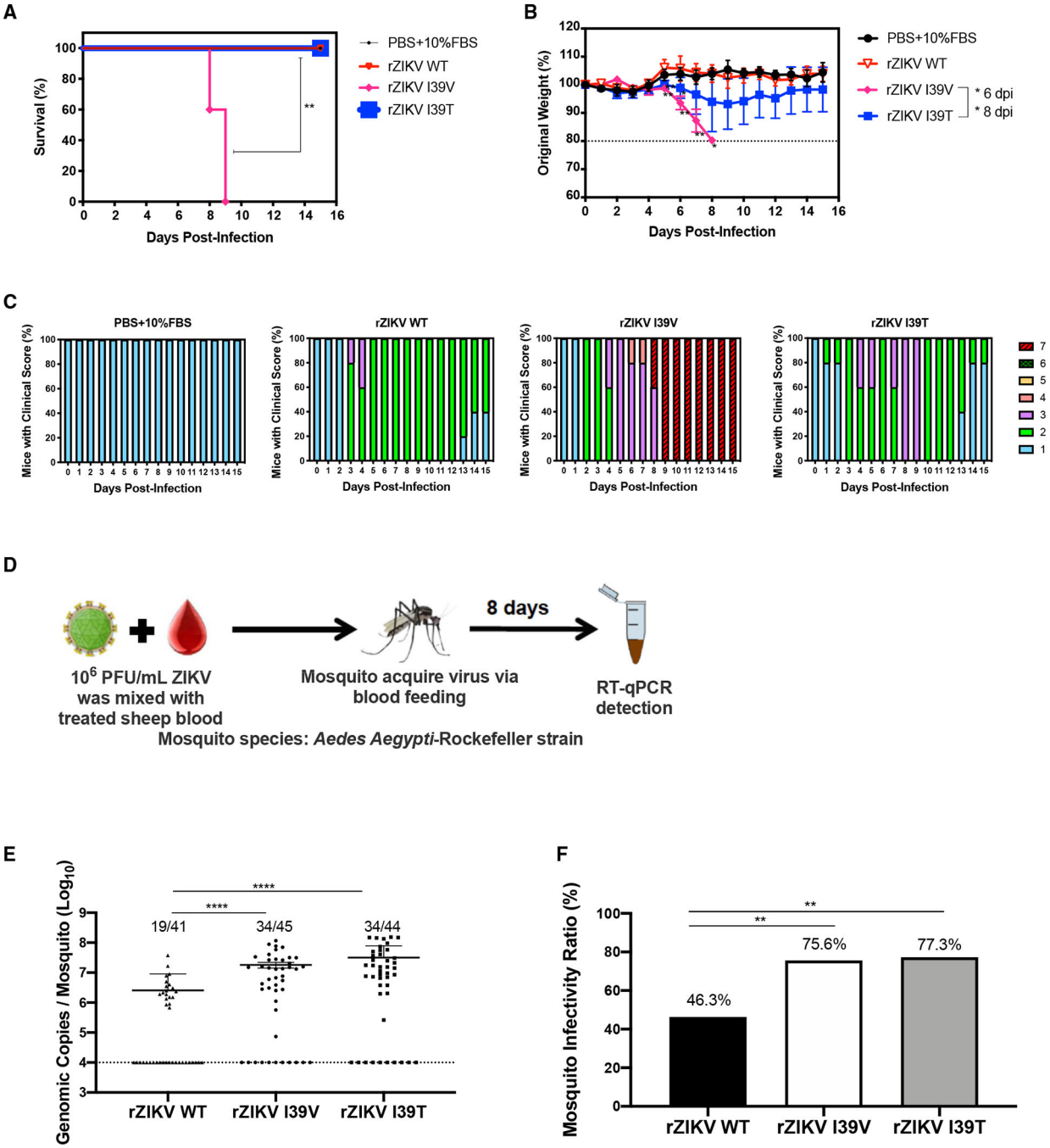

Figure 4. I39V and I39T mutations differentially affect ZIKV virulence in DENV-immune *Ifnar1*$^{-/-}$ mice but both mutations enhance ZIKV fitness for transmission and replication in mosquitoes

(A–C) DENV2-immune *Ifnar1*$^{-/-}$ mice were generated by intraperitoneal injection of 10^3 FFU DENV2 strain S221 for 30 days, and groups of mice were then injected intra-footpad with PBS/10% FBS or 10^4 FFU of rZIKV-WT, rZIKV-NS2B-I39V, or rZIKV-NS2B-I39T strains. Animals were monitored daily for survival (A), weight loss (B), and clinical score (C). Animals that lost >20% of their initial body weight were euthanized (n = 5 mice/group).

(D) Experimental scheme for infection of mosquitoes via simulated blood feeding. *A. aegypti* (Rockefeller) mosquitoes were allowed to feed for 30 min on a sheep blood–virus mixture containing 10^6 PFU/mL of rZIKV-WT, rZIKV-NS2B-I39V, or rZIKV-NS2B-I39T strains using the Hemotek membrane blood-feeding system. Eight days later, mosquitoes were analyzed.

(E) RT-qPCR quantification of rZIKV RNA levels normalized to mosquito actin mRNA levels. Dotted line indicates the threshold for designation as infected (10^4 genomic copies/mosquito), which was used for calculating the infectivity rates in (F). Data are presented as the mean ± SEM of the indicated number of mosquitoes and were pooled from two independent experiments (symbols represent individual mosquitoes).

(F) Percentage mosquito infectivity ratios ([infected number/total number] × 100). Data are presented as the mean ± SEM and were pooled from two independent experiments. *$p < 0.05$, **$p < 0.01$, ****$p < 0.0001$ by Gehan–Breslow–Wilcoxon test (survival), two-tailed Mann–Whitney test (body weights and genomic copies/mosquito) and Fisher's exact test (mosquito infectivity ratio).

KEY RESOURCES TABLE

REAGENT or RESOURCE	SOURCE	IDENTIFIER
Antibodies		
Pan-flavivirus envelope protein-specific monoclonal antibody 4G2 Absolute Antibody (clone D1-4G2-4-15)	Absolute Antibody	Cat#Ab00230-2.0; RRID: AB_2715504
Peroxidase conjugated affini-pure goat anti-mouse IgG Fc γ	Jackson ImmunoResearch	Cat. #115-035-008; RRID: AB_2313585
Bacterial and virus strains		
ZIKV FSS13025 (Cambodia, 2010)	WRCEVA, (Galveston, TX)	N/A
DENV2 (S221)	(Yauch et al., 2009)	N/A
Chemicals, peptides, and recombinant proteins		
Carboxymethyl cellulose	Sigma-Aldrich	Cat#9004-32-4
TrueBlue peroxidase substrate	KPL	Cat#5510-0030
ZIKV E protein	The Native Antigen	N/A
Qiamp Viral Mini Kit	Qiagen	Cat. #52904
RNAlater	Thermo Fisher Scientific	Cat. #AM7021
QuantaBio qScript one-step qRT-PCR kit	VWR	Cat. #101414-172
StemProTM AccutaseTM Cell Dissociation Reagent	Thermo Fisher Scientific	Cat. #A1110501
Experimental models: Cell lines		
Baby hamster kidney (BHK)-21 cells	ATCC	Cat. #ATCC: CCL-10 RRID: CVCL_1915
Aedes albopictcus: C6/36 cells	ATCC	Cat. #ATCC: CRL-1660 RRID: CVCL_Z230
Vero cells	ATCC	(CRL-1586)
Human fetal neural progenitor cells (NPCs)	A. V. Terskikh	N/A
Experimental models: Organisms/strains		
Ifnar1$^{-/-}$ mice (C57BL/6 background) (males and females)	(Yauch et al., 2009)	N/A
BALB/c mice (males)	Jackson Labs	Cat. #000651
Aedes aegypti mosquitoes (Rockefeller strain)	P.-Y. Shi	N/A
Oligonucleotides		
Primers used for construction of recombinant ZIKV viruses	Table S1	N/A
Primers and probes used for determination of ZIKV viral burden	Table S2	N/A
Other		
KPL True Blue	SeraCare	Cat. #5510-0030
Leibovitz's L-15	Thermo Fisher Scientific	Cat. #11415064
Fetal bovine serum (FBS)	Thermo Fisher Scientific	Cat. #16000044
Penicillin/streptomycin	Thermo Fisher Scientific	Cat. #15140122
HEPES	Thermo Fisher Scientific	Cat. #15630080

REAGENT or RESOURCE	SOURCE	IDENTIFIER
High-glucose Dulbecco's modified Eagle's medium	Thermo Fisher Scientific	Cat. #11995065
DMEM/F12	Corning	Cat. #10-092-CV
N-2 supplement	Thermo Fisher Scientific	Cat. #17502048
B-27™ supplement (50X), minus vitamin A	Thermo Fisher Scientific	Cat. #12587010
human FGF-basic	Thermo Fisher Scientific	Cat. #PHG0263
MEM non-essential amino acids solution	Thermo Fisher Scientific	Cat. #11140050
Formalin	Fisher	Cat. #SF98-4
Triton X-100	Sigma	Cat. #X100-100ML
RNeasy Mini Kit	Qiagen	Cat. #73404
AvrII	(New England BioLabs)	Cat. #R0174S
SphI	(New England BioLabs)	Cat. #R0182S
NaeI	(New England BioLabs)	Cat. #R0190S
ClaI	(New England BioLabs)	Cat. #R0197S
mMESSAGE mMACHINE™ T7 transcription kit	(Thermo Fisher Scientific)	Cat. #AM1344
Complement-inactivated sheep blood	(Hemostat laboratories)	Cat. #C26218